2.4. Powder and related techniques: electron and neutron techniques

By J. M. Cowley and A. W. Hewat

2.4.1. Electron techniques (By J. M. Cowley)

2.4.1.1. *Powder-pattern geometry*

The electron wavelengths normally used to obtain powder patterns from thin films of polycrystalline materials lie in the range 8×10^{-2} to 2×10^{-2} Å (20 to 200 kV accelerating voltages). The maximum scattering angles ($2\theta_B$) observed are usually less than 10^{-1} rad.

Patterns are usually recorded on flat photographic plates or films and a small-angle approximation is applied. For a camera length L, the distance from the specimen to the photographic plate in the absence of any intervening electron lenses, the approximation is made that, for a diffraction ring of radius r,

$$\lambda/d = 2\sin\theta \simeq \tan 2\theta = r/L,$$

or the interplanar spacing, d, is given by

$$d = L\lambda/r. \qquad (2.4.1.1)$$

For a scattering angle of 10^{-1} rad, the error in this expression is 0.5%. A better approximation, valid to better than 0.1% at 10^{-1} rad, is

$$d = (L\lambda/r)(1 + 3r^2/8L^2). \qquad (2.4.1.2)$$

The 'camera constant' $L\lambda$ may be obtained by direct measurement of L and the accelerating voltage if there are no electron lenses following the specimen.

Direct electronic recording of intensities has great advantages over photographic recording (Tsypursky & Drits, 1977).

In recent years, electron diffraction patterns have been obtained most commonly in electron microscopes with three or more post-specimen lenses. The camera-constant values are then best obtained by calibration using samples of known structure.

With electron-optical instruments, it is possible to attain collimations of 10^{-6} rad so that for scattering angles of 10^{-1} rad an accuracy of 10^{-5} in d spacings should be possible in principle but is not normally achievable. In practice, accuracies of about 1% are expected. Some factors limiting the accuracy of measurement are mentioned in the following sections. The small-angle-scattering geometry precludes application of any of the special camera geometries used for high-accuracy measurements with X-rays (Chapter 2.3).

2.4.1.2. *Diffraction patterns in electron microscopes*

The specimens used in electron microscopes may be self-supporting thin films or fine powders supported on thin films, usually made of amorphous carbon. Specimen thicknesses must be less than about 10^3 Å in order to avoid perturbations of the diffraction patterns by strong multiple-scattering effects. The selected-area electron-diffraction (SAED) technique [see Section 2.5.1 in *IT* B (1993)] allows sharply focused diffraction patterns to be obtained from regions 10^3 to 10^5 Å in diameter. For the smaller ranges of selected-area regions, specimens may give single-crystal patterns or very spotty ring paterns, rather than continuous ring patterns, because the number of crystals present in the field of view is small unless the crystallite size is of the order of 100 Å or less. By use of the convergent-beam electron-diffraction (CBED) technique, diffraction patterns can be obtained from regions of diameter 100 Å [see Section 2.5.2 in *IT* B (1993)] or, in the case of some specialized instruments, regions less than 10 Å in diameter. For these reasons, the methods for phase identification from electron diffraction patterns and the corresponding databases (see Subsection 2.4.1.6) are increasingly concerned with single-crystal spot patterns in addition to powder patterns.

Instrument manufacturers usually provide values of camera lengths, L, or camera constants, $L\lambda$, for a wide range of designated lens-current settings. It is advisable to check these calibrations with samples of known structure and to determine calibrations for non-standard lens settings.

The effective camera length, L, is dependent on the specimen height within the objective-lens pole-piece. If a specimen-height adjustment (a z-lift) is provided, it should be adjusted to give a predetermined lens current, and hence focal length, of the objective lens.

In some microscopes, at particular lens settings the projector lenses may introduce a radial distortion of the diffraction pattern. This may be measured with a suitable standard specimen.

2.4.1.3. *Preferred orientations*

The techniques of specimen preparation may result in a strong preferred orientation of the crystallites, resulting in strong arcing of powder-pattern rings, the absence of some rings, and perturbations of relative intensities.

For example, small crystals of flaky habit deposited on a flat supporting film may be oriented with one reciprocal-lattice axis preferentially perpendicular to the plane of the support. A ring pattern obtained with the incident beam perpendicular to the support then shows only those rings for planes in the zone parallel to the preferred axis. Such orientation is detected by the appearance of arcing and additional reflections when the supporting film is tilted. Tilted specimens give the so-called oblique texture patterns which provide a rich source of three-dimensional diffraction information, used as a basis for crystal structure analysis.

A full discussion of the texture patterns resulting from preferred orientations is given in Section 2.5.3 of *IT* B (1993).

2.4.1.4. *Powder-pattern intensities*

In the kinematical approximation, the expression for intensities of electron diffraction follows that for X-ray diffraction with the exception that, because only small angles of diffraction are involved, no polarization factor is involved. Following Vainshtein (1964), the intensity per unit length of a powder line is

$$I(h) = J_0\lambda^2 \left| \frac{\Phi_h}{\Omega} \right|^2 V \frac{d_h^2 M}{4\pi L\lambda}, \qquad (2.4.1.3)$$

where J_0 is the incident-beam intensity, Φ_h is the structure factor, Ω is the unit-cell volume, V is the sample volume, and M is the multiplicity factor.

The kinematical approximation has limited validity. The deviations from this approximation are given to a first approximation by the two-beam approximation to the dynamical-scattering theory. Because an averaging over all orientations is involved, the many-beam dynamical-diffraction effects are less evident than for single-crystal patterns.

By integrating the two-beam intensity expression over excitation error, Blackman (1939) obtained the expression for the ratio of dynamical to kinematical intensities:

$$I_{\rm dyn}/I_{\rm kin} = A_h^{-1} \int_0^{A_h} J_0(2x)\,{\rm d}x, \qquad (2.4.1.4)$$

where $J_o(x)$ is the zero-order Bessel function, $A_h = \sigma H \Phi_h$ with the interaction constant $\sigma = 2\pi me\lambda/h^2$, and H is the crystal thickness. Careful measurements on ring patterns from thin aluminium films by Horstmann & Meyer (1962) showed agreement with the 'Blackman curve' [from equation (2.4.1.4)] to within about 5% with some notable exceptions. Deviations of up to 40 to 50% from the Blackman curve occurred for several reflections, such as 222 and 400, which are second-order reflections from strong inner reflections. A practical algorithm for implementing Blackman corrections has been published by Dvoryankina & Pinsker (1958).

Such deviations result from plural-beam *systematic interactions*, the coherent multiple scattering between different orders of a strong inner reflection. When the Bragg condition is satisfied for one order, the excitation errors for the other orders are the same for all possible crystal orientations and these other orders contribute systematically to the ring-pattern intensities. A correction for the effects of systematic interactions may be made by use of the Bethe second approximation (Bethe, 1928) (see Chapter 8.8).

For non-systematic reflections, corresponding to reciprocal-lattice points not collinear with the origin and the reciprocal-lattice point of interest, the averaging over all crystal orientations ensures that the powder-pattern intensity calculated from the two-beam formula will not be appreciably affected. Appreciable effects from non-systematic interactions may, however, occur when the averaging is over a limited range of crystal orientations, as in the case of strong preferred orientations. It was shown theoretically by Turner & Cowley (1969) and experimentally by Imamov, Pannhorst, Avilov & Pinsker (1976) that appreciable modifications of intensities of oblique-texture patterns may result from non-systematic interactions for particular tilt angles, especially for heavy-atom materials [see also Avilov, Parmon, Semiletov & Sirota (1984)].

The techniques for the measurement of electron diffraction intensities are described in Chapter 7.2. Most commonly electron diffraction powder patterns are recorded by photographic methods and a microdensitometer is used for quantitative intensity measurement. The Grigson scanning method, using a scintillator and photomultiplier to record intensities as the pattern is scanned over a fine slit, has considerable advantages in terms of linearity and range of the intensity scale (Grigson, 1962). This method also has the advantage that it may readily be combined with an energy filter so that only elastically scattered electrons (or electrons inelastically scattered with a particular energy loss) may be recorded.

Small-angle electron diffraction may give useful information in some cases, but must be interpreted carefully because the features may result from multiple scattering or other artefacts. It may give additional details of periodicity (super-periods) and deviations of the real symmetry from the ideal symmetry suggested by other data. Care must be taken with the interpretation of additional reflections, as they may relate to the structure of small regions that are not typical of the bulk specimens such as are examined by X-ray diffraction.

The techniques for interpretation of electron diffraction powder-pattern intensities follow those for X-ray patterns when the kinematical approximation is valid. For very small crystals, giving very broad rings, it is possible to use the method, commonly applied for diffraction by gases, of performing a Fourier transform to obtain a radial distribution function (Goodman, 1963).

2.4.1.5. *Crystal-size analysis*

The methods used in X-ray diffraction for the determination of average crystal size or size distributions may be applied to electron diffraction powder patterns. Except in the case of very small crystal dimensions, several factors peculiar to electrons should be taken into consideration.

(*a*) Unless energy filtering is used to remove inelastically scattered electrons, a component is added to the rings broadened by the effects of inelastic scattering involving electronic excitations. Since the mean free paths for such processes are of the order of 10^3 Å and the angular spread of the scattered electrons is 10^{-3} to 10^{-4} rad, the ring broadening for thick samples may be equivalent to the broadening for a crystal size of the order of 100 Å.

(*b*) When a powder sample consists of separated crystallites having faces not predominantly parallel or perpendicular to the incident beam, the diffraction rings may be appreciably broadened by refraction effects. The refractive index for electrons is given, to a first approximation, by

$$n = 1 + \Phi_0/2E,$$

where Φ_0 is the mean inner potential of the crystal, typically 10 to 20 V, and E is the accelerating voltage of the incident electron beam. For the beam passing through the two faces of a 90° wedge, each at an angle $\alpha = 45°$ to the beam, for example, the beam is deflected by an amount

$$\Delta = \Phi_0/E = 1.5 \times 10^{-4}\ {\rm rad}$$

for an inner potential of 15 V and $E = 100$ kV. The broadening of the ring by such deflections can correspond to the broadening due to a particle size of $\lambda/2\Delta \simeq 120$ Å.

For crystallites of regular habit, such as the small cubic crystals of MgO smoke, the ring broadening from this source is strongly dependent on the crystallographic planes involved (Sturkey & Frevel, 1945; Cowley & Rees, 1947; Honjo & Mihama, 1954). For more isometric crystal shapes, this dependence is less marked and the broadening has been estimated (Cowley & Rees, 1947) as equivalent to that due to a particle size of about 200 Å.

2.4.1.6. *Unknown-phase identification: databases*

To a limited extent, the compilations of data for X-ray diffraction, such as the ICDD Powder Diffraction File, may be used for the identification of phases from electron diffraction data. The nature of the electron diffraction data and the circumstances of its collection have prompted the compilation of databases specifically for use with electron diffraction. Factors taken into consideration include the following.

(*a*) Because of the increasing use of single-crystal patterns obtained in the SAED mode in an electron microscope, the use of single-crystal spot patterns, in addition to powder patterns, must be considered for purposes of identification. Methods for the analysis of single-crystal patterns are summarized in Section 5.4.1.

(*b*) The deviations from kinematical scattering conditions may be large, especially for single-crystal patterns, so that little reliance can be placed on relative intensities, and reflections kinematically forbidden may be present.

(*c*) Compositional information may be obtained by use of X-ray microanalysis (or electron-energy-loss spectroscopy) performed in the electron microscope and this provides an effective additional guide to identification.

(*d*) Electron diffraction data often extend to smaller *d* spacings than X-ray data because there is no wavelength limitation.

(*e*) The electron diffraction *d*-spacing information is rarely more precise than 1% and the uncertainty may be 5% for large *d* spacings.

With these points in mind, databases specially designed for use with electron diffraction have been developed. The NIST/Sandia/ICDD Electron Diffraction Database follows the design principles of Carr, Chambers, Melgaard, Himes, Stalick & Mighell (1987). The 1993 version contains crystallographic and chemical information on over 81 500 crystalline materials with, in most cases, calculated patterns to ensure that diagnostic high-*d*-spacing reflections can be matched. It is available on magnetic tape or floppy disks. The MAX-d index (Anderson & Johnson, 1979) has been expanded to 51 580 NSI-based entries (Mighell, Himes, Anderson & Carr, 1988) in book form for manual searching.

2.4.2. Neutron techniques (By A. W. Hewat)

Neutrons have advantages over X-rays for the refinement of crystal structures from powder data because systematic errors (Wilson, 1963) are smaller, and the absence of a form factor means that information is available at small *d* spacings. It is also easy to collect data at very low or high temperature; examining the structure as a function of temperature (or pressure) is much more useful than simply obtaining 'the' crystal structure at STP (standard temperature and pressure). In some cases, 'kinetics' measurements at intervals of only a few seconds are needed to follow chemical reactions.

A neutron powder diffractometer need not separate all of the Bragg peaks, since complex patterns can be analysed by Rietveld refinement (Rietveld, 1969), but high resolution will increase the information content of the profile, and permit the refinement of larger and more complex structures. Doubling the unit-cell volume doubles the number of Bragg peaks, requiring higher resolution, but also halves the average peak intensity. Resolution must not then be obtained at the expense of well defined line shape, essential for profile analysis, nor at the expense of intensity.

Two types of diffractometer are required in practice: a high-resolution machine with data-collection times of a few hours (or days) for Rietveld structure refinement, and a high-flux machine with data-collection times of a few seconds (or minutes) for kinetics measurements. In both cases, the data-collection rate depends on the product of the flux on the sample, the sample volume, and the solid angle of the detector (Hewat, 1975). The flux on the sample can be increased with a focusing monochromator, the sample volume by using large sample-detector distances or Soller collimators, and the detector solid angle by using a large multidetector.

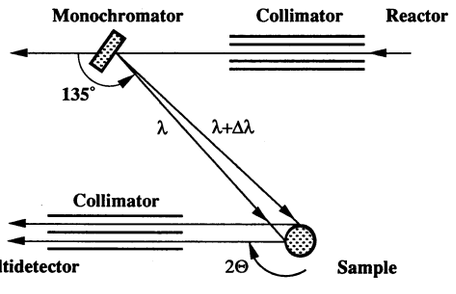

Fig. 2.4.2.1. Schematic drawing of the high-resolution neutron powder diffractometer D2B at ILL, Grenoble.

The focusing monochromator is usually made from horizontal strips of pyrolytic graphite or squashed germanium mounted on a vertically focusing plate 100 to 300 mm high. A large beam can thus be focused on a sample up to 50 mm high. Vertical divergence of 5° or more can be tolerated even for a high-resolution machine; the peak width is only increased (and made asymmetric) far from scattering angles of 90°, where most of the peaks occur. The effect is in any case purely geometrical, and can readily be included in the data analysis (Howard, 1982).

To increase the wavelength spread $\Delta\lambda/\lambda$, and hence intensity, monochromator mosaic can be large (20′) even for high resolution, since all wavelengths are focused back into the primary-beam direction at scattering angles equal to the monochromator take-off angle (Fig. 2.4.2.1).

Rather long wavelengths (1.5 to 3 Å) are favoured, to spread out the pattern, and to reduce the total number of reflections excited (increasing their average intensity). Data must then be collected at large scattering angles with good resolution to obtain sufficiently small *d* spacings, and this implies a large take-off angle. A graphite filter to remove $\lambda/2$ and higher-order contamination is a popular choice for a primary wavelength of 2.4 Å (Loopstra, 1966). Since germanium reflections such as *hhl* with h, $l = 2n + 1$ do not produce $\lambda/2$ contamination, a filter is not needed for primary wavelengths below about 1.6 Å with high-take-off-angle geometry, but is still necessary for longer wavelengths.

The multidetector can be an array of up to 64 individual detectors and Soller collimators for a high-resolution machine (Hewat & Bailey, 1976; Hewat, 1986*a*), or a position-sensitive detector (PSD) for a high-flux machine (Allemand *et al.*, 1975). Gas-filled (^{3}He or BF_3) detectors are usual, though scintillator and other types of solid-state detector are increasingly used; the PSD may be either a single horizontal wire with position-detection logic comparing the signals obtained at either end, or an array of vertical wire detectors within a common gas envelope. The vertical aperture of the single-wire detector seriously limits the efficiency of what is otherwise a very cheap solution, and of course large angular ranges cannot be covered by a single straight wire.

The vertical aperture should match the vertical divergence from the monochromator ($\sim 5°$). Composite detectors can be constructed by stacking elements both vertically to increase the aperture, and horizontally to increase the angular range. Construction of a wide-angle (160°) multiwire detector is difficult and expensive, but a solid angle of more than 0.1 sr may be obtained. The solid angle for a collimated multidetector, even if it covers 160°, may be less than 0.01 sr.

The sample volume limits the resolution of the PSD, since the detector resolution α_3 (typically 0.2°) is the mean of the element width and the sample diameter (typically 5 mm) divided by the sample-to-detector distance (typically 1500 mm). For a Soller collimator, α_3 can be as little as 5′, and does not depend on the sample volume, which can be large (20 mm diameter) even for high resolution. The PSD also requires special precautions to avoid background from the sample environment, while the collimated machine can handle difficult sample environments, especially for scattering near 90°.

The definition of the detector is the number of data points per degree. For profile analysis, unless the peak shape is well known *a priori*, about five points are needed per reflection half-width, which is more than usually available from a multiwire PSD.

However, a PSD may be scanned to increase the profile definition. The minimum scan angle is clearly the angle between elements, from 0.2° for a PSD to 2.5° or more for a multidetector in steps of from 0.025 to 0.1°. If larger scans are performed, it is most convenient to reduce the data to a single profile by averaging the counts from different detector elements at each point in the profile, after correcting for relative efficiencies and angular separations.

The resolution, of either machine, should be no better than really necessary for a particular sample: additional resolution merely reveals problems with sample perfection and line shape, making Rietveld refinement difficult, and of course reducing effective intensity. In any case, resolution is ultimately limited by the powder particle size and strain broadening (Hewat, 1975). As an order of magnitude, if $D = 1000$ Å is the effective size of the perfect crystallites that make up a much larger (1 to 10 μm) powder grain, then for lattice spacing $d = 1$ Å, the best resolution that one can hope to obtain is of the order $\Delta d/d = d/D = 10^{-3}$, corresponding to a line width of $\Delta(2\theta) \simeq 0.1°$. A few more perfect materials (usually those for which single crystals can be grown!) will produce higher-resolution patterns, but then primary extinction may not be negligible.

It is not even necessary to have the best possible resolution for all d spacings: ideally, the resolution should be proportional to the density of lines, and this increases with the surface area of the Ewald sphere of radius $1/d$. Then we want $\Delta d/d = d^2$ or $\Delta(2\theta) = \lambda^2/\sin 2\theta$. This has a minimum near $2\theta = 90°$. In fact, the full width at half-height is (Cagliotti, Paoletti & Ricci, 1958)

$$\Delta^2(2\theta) = U\tan^2\theta + V\tan\theta + W.$$

The parameters U, V, and W are functions of the monochromator mosaic spread and collimation, from which it follows that the minimum in $\Delta(2\theta)$ occurs for scattering angles $2\theta \simeq 2\theta_M$. The monochromator take-off angle should then be at least 90°; in practice, since $\Delta^2(2\theta)$ increases quadratically with $\tan\theta$ for angles larger than this focusing angle, the monochromator take-off should be even greater than 90°. A value of 120 to 135° is recommended.

For this focusing geometry, the different wavelengths $\lambda + \Delta\lambda$, reflected at different angles from the monochromator, are brought back parallel to the primary beam, and the line width becomes simply the convolution of the primary and detector collimations α_1 and α_3:

$$\Delta^2(2\theta) = \alpha_1^2 + \alpha_3^2.$$

The collimators α_1 and α_3 should then be equal and small. Such fine collimators are now made routinely from gadolinium oxide-coated stretched plastic foil (Carlile, Hey & Mack, 1977). The collimator α_2 should simply be large enough to pass all wavelengths reflected by the mosaic spread β of the monochromator, *i.e.* $\alpha_2 \simeq 2\beta$.

Neutron crystallographers have been reluctant to use large take-off angles because they seem to imply greatly reduced beam intensity. Indeed, large θ_M means small waveband $\Delta\lambda/\lambda$ since $\Delta\lambda/\lambda = \Delta d/d = \Delta(\theta_M)\cot\theta_M = \beta\cot\theta_M$. However, $\Delta\lambda/\lambda$ and therefore beam intensity can be recovered simply by increasing β. This has no effect on the resolution at focusing, but it does increase the line width at low angles where there are few lines. When large d spacings are needed, for example for magnetic structures, it is best for both resolution and intensity to retain the same high take-off geometry and increase the wavelength to bring these lines closer to the focusing angle. A large take-off angle also gives a large choice of high-index reflections and wavelengths up to 6 Å!

A fixed take-off angle greatly simplifies machine design: the multidetector collimation α_3 is also necessarily fixed, but the single primary collimator α_1 can readily be changed. It is useful to have a second choice, much larger than α_3, to boost intensity for poor samples or exploratory data collection. The resolution at low angles, largely determined by β (or α_2), is not much affected by increasing α_1.

Finally, the machine should be designed around the sample environment, since this is one of the strengths of neutron powder diffraction. There is no point in building a neutron machine with superb resolution and intensity (these can much more readily be obtained with X-rays) if it cannot produce precise results for the kind of experiments of most interest – those for which it is difficult to use any other technique (Hewat, 1986*b*).

2.4.1

Anderson, R. & Johnson, G. G. Jr (1979). *The MAX-d alphabetical index to the JCPDS data base: a new tool for electron diffraction analysis. 37th Annu. Proc. Electron Microsc. Soc. Am.*, edited by G. W. Bailey, pp. 444–445. Baton Rouge: Claitors.

Avilov, A. S., Parmon, V. S., Semiletov, S. A. & Sirota, M. I. (1984). *Intensity calculations for many-wave diffraction of fast electrons in polycrystal specimens. Kristallografiya*, **29**, 11–15. [In Russian.]

Bethe, H. A. (1928). *Theorie der Beugung von Elektronen an Kristallen. Ann. Phys. (Leipzig)*, **87**, 55–129.

Blackman, M. (1939). *On the intensities of electron diffraction rings. Proc. R. Soc. London*, **173**, 68–82.

Carr, M. J., Chambers, W. F., Melgaard, D. K., Himes, V. L., Stalick, J. K. & Mighell, A. D. (1987). *NBS/Sandia/ICDD Electron Diffraction Data Base*. Report SAND87-1992-UC-13. Sandia National Laboratories, Albuquerque, NM 87185, USA.

Cowley, J. M & Rees, A. L. G. (1947). *Refraction effects in electron diffraction. Proc. Phys. Soc.* **59**, 287–302.

Dvoryankina, G. G. & Pinsker, Z. G. (1958). *The structural study of Fe_4N. Kristallografiya*, **3**, 438–445. [In Russian.]

Goodman, P. (1963). *Investigation of arsenic trisulphide by the electron diffraction radial distribution method. Acta Cryst.* **16**, A130.

Grigson, C. W. B. (1962). *On scanning electron diffraction. J. Electron. Control,* **12**, 209–232.

Honjo, G. & Mihama, K. (1954). *Fine structure due to refraction effect in electron diffraction pattern of powder sample. J. Phys. Soc. Jpn*, **9**, 184–198.

Horstmann, M. & Meyer, G. (1962). *Messung der Elastischen Electronenbeugungsintensitaten polykristalliner Aluminium-Schichten. Acta Cryst.* **15**, 271–281.

Imamov, R. M., Pannhorst, V., Avilov, A. S. & Pinsker, Z. G. (1976). *Experimental study of dynamic effects associated with electron diffraction in partly oriented films. Kristallografiya*, **21**, 364–369.

International Tables for Crystallography (1993). Vol. B. Dordrecht: Kluwer Academic Publishers.

Mighell, A. D., Himes, V. L., Anderson, R. & Carr, M. J. (1988). *d-spacing and formula index for compound identification using electron diffraction. 46th Annu. Proc. Electron Microsc. Soc. Am.*, edited by G. W. Bailey, pp. 912–913. San Francisco Press.

Sturkey, L. & Frevel, L. K. (1945). *Refraction effects in electron diffraction. Phys. Rev.* **68**, 56–57.

Tsypursky, S. I. & Drits, V. A. (1977). *The efficiency of the electronometric measurement of intensities in electron diffraction structural studies. Izv. Akad. Nauk SSSR Ser. Phys.* **41**, 2263–2271. [In Russian.]

Turner, P. S. & Cowley, J. M. (1969). *The effect of n-beam dynamical diffraction in electron diffraction intensities from polycrystalline materials. Acta Cryst.* A**25**, 475–481.

Vainshtein, B. K. (1964). *Structure analysis by electron diffraction*. Oxford: Pergamon Press. [Translated from the Russian: *Strukturnaya Electronografiya*.]

2.4.2

Allemand, R., Bordet, J., Roudaut, E., Convert, P., Ibel, K., Jacobe, J., Cotton, J. P. & Farnoux, B. (1975). *Position sensitive detectors for neutron diffraction. Nucl. Instrum. Methods*, **126**, 29–42.

Caglioti, G., Paoletti, A. & Ricci, F. P. (1958). *Choice of collimators for a crystal spectrometer for neutron diffraction. Nucl. Instrum. Methods*, **3**, 223–228.

Carlile, C. J., Hey, P. D. & Mack, B. (1977). *High efficiency Soller slit collimators for thermal neutrons. J. Phys. E*, **10**, 543–546.

Hewat, A. W. (1975). *Design for a conventional high resolution neutron powder diffractometer. Nucl. Instrum. Methods*, **127**, 361–370.

Hewat, A. W. (1986*a*). *D2B, a new high resolution neutron powder diffractometer at ILL Grenoble. Mater. Sci. Forum*, **9**, 69–79.

Hewat, A. W. (1986*b*). *High resolution neutron and synchrotron powder diffraction. Chem. Scr.* **26**A, 119–130.

Hewat, A. W. & Bailey, I. (1976). *D1A, a high resolution neutron powder diffractometer with a bank of Mylar collimators. Nucl. Instrum. Methods*, **137**, 463–471.

Howard, C. J. (1982). *The approximation of asymmetric neutron powder diffraction peaks by sums of Gaussians. J. Appl. Cryst.* **15**, 615–620.

Loopstra, B. O. (1966). *Neutron powder diffractometry using a wavelength of 2.6 Å. Nucl. Instrum. Methods*, **44**, 181–187.

Rietveld, H. M. (1969). *A profile refinement method for nuclear and magnetic structures. J. Appl. Cryst.* **2**, 65–71.

Wilson, A. J. C. (1963). *Mathematical theory of X-ray powder diffractometry*. Eindhoven: Centrex.

2.5.1

Besson, J. M. & Weill, G. (1992). *EDX station for high pressure at LURE (DCI). High Press. Res.* **8**, 715–716.

Bourdillon, A. J., Glazer, A. M., Hidaka, M. & Bordas, J. (1978). *High-resolution energy-dispersive diffraction using synchrotron radiation. J. Appl. Cryst.* **11**, 684–687.

Buras, B., Chwaszczewska, J., Szarras, S. & Szmid, Z. (1968). *Fixed angle scattering* (*FAS*) *method for X-ray crystal structure analysis*. Report No. 894/II/PS, 10 pp. Institute of Nuclear Research, Warsaw.

Buras, B. & Gerward, L. (1975). *Relations between integrated intensities in crystal diffraction methods for X-rays and neutrons. Acta Cryst.* A**31**, 372–374.

Buras, B. & Gerward, L. (1989). *Application of X-ray energy-dispersive diffraction for characterization of materials under high pressure. Prog. Cryst. Growth Charact.* **18**, 93–138.

Buras, B., Gerward, L., Glazer, A. M., Hidaka, M. & Olsen, J. S. (1979). *Quantitative structural studies by means of the energy-dispersive method with X-rays from a storage ring. J. Appl. Cryst.* **12**, 531–536.

Buras, B., Niimura, N. & Olsen, J. S. (1978). *Optimum resolution in X-ray energy-dispersive diffractometry. J. Appl. Cryst.* **11**, 137–140.

Buras, B., Olsen, J. S., Gerward, L., Selsmark, B. & Lindegaard-Andersen, A. (1975). *Energy-dispersive spectroscopic methods applied to X-ray diffraction in single crystals. Acta Cryst.* A**31**, 327–333.

Clark, S. M. (1992). *A new white beam single crystal and powder diffraction facility at the SRS. Rev. Sci. Instrum.* **63**, 1010–1012.

Fukamachi, T., Hosoya, S. & Terasaki, O. (1973). *The precision of interplanar distances measured by an energy-dispersive method. J. Appl. Cryst.* **6**, 117–122.